Investigation of Formation Channels of Mass-Gap Black Holes from Spin Distributions

Jeehoo Shin[1]

Received September 3, 2025
Accepted February 20, 2026
Electronic access March 15, 2026

The lower mass gap spans approximately 2.5 to 5 $M_\odot$ and represents a region in the compact object mass spectrum that is not yet fully understood. However, with recent LIGO-Virgo-KAGRA gravitational-wave observations, the lower mass gap has populated with several new candidate events, offering new opportunities to investigate the formation mechanisms of these complex compact objects. This study analyses the effective inspiral spin parameter $\chi_{\rm eff}$ for the gravitational-wave merger events containing at least one component within the lower mass gap, using posterior samples from the GWTC-3 catalogue. I find that the population mean effective spin is consistent with zero ($\mu = 0.028^{+0.069}_{-0.049}$), indicating predominantly isotropic spin orientations. This result suggests a preference for dynamical assembly formation channels over isolated binary evolution, as the latter typically form preferentially aligned positive spins values. The isotropic spin distribution implies that these compact objects are formed through gravitational encounters in dense stellar environments such as globular clusters or nuclear star clusters. These findings further contribute to resolving the nature of the lower mass gap and provide observational constraints on compact object formation pathways. While the sample size limits statistical precision, the results are consistent with theoretical predictions for dynamically assembled binaries.

Introduction

Black holes are dense remnants left behind by the collapse of massive stars[1]. Their defining characteristic of an event horizon prevents light from escaping, meaning that they must be observed through their effects on surrounding matter and spacetime. For decades, compact objects have been identified through X-ray binaries, where a black hole accretes matter from a companion star, producing X-rays emission[2,3]. Theoretical models and recent observations have shown that compact objects fall into several broad populations. The common groups are white dwarfs with masses up to 1.4 $M_\odot$ (Chandrasekhar limit), neutron stars with an approximate mass below 2.5 $M_\odot$, and black holes of varying masses depending on their formation and evolution history. While white dwarfs are common, the current gravitational-wave detectors are not sensitive to their merger signatures. The nature of the lower mass gap between 2.5 to 5 $M_\odot$ range is uncertain. Fryer & Kalogera[4] suggested two possible reasons for this mass gap: a physical origin involving the mechanisms of collapsing supernovae that fail to produce a remnant within the range, or a selection bias against the identification of low-mass black holes. The true origin of the lower mass gap is yet to be confirmed. However, the developing technology of gravitational-wave detection offers a new opportunity to observe and investigate these compact objects.

Unlike X-ray surveys, gravitational-wave detectors such as LIGO[5]and Virgo[6] can detect the merger of compact objects regardless of their electromagnetic output. Several events with at least one black hole falling into the mass gap have been observed and are now listed in the Gravitational Wave Open Science Center (GWOSC) catalogue[7–9]. These observations provide an alternative means to determine whether such compact objects exist and, if so, the origins of their formation. In the case that such compact objects exist, two main formation channels are thought to dominate current models. The first formation channel, isolated binary evolution, occurs when two gravitationally bound compact objects form and evolve together in a binary system. Over time, these stars undergo processes such as mass transfer, common-envelope evolution, or supernova explosions, eventually leaving behind two compact objects of either a black hole or neutron star. The system evolves in isolation and is not significantly affected by external forces. Thus, the spins of the objects remain aligned with the orbital angular momentum, leading to positive effective inspiral spin values[10]. The effective inspiral spin is a parameter that measures the mass-weighted alignment of the component spins with the orbital axis, indicating whether the spins are more aligned or randomly oriented. Conversely, dynamical assembly occurs in denser stellar environments such as globular clusters or galactic nuclei. In these regions, black holes and other compact objects frequently interact and undergo a series of mass transfers or mergers. After many interactions, a

[1] *British School Jakarta*

final binary system forms. Unlike the isolated binary system, these binaries have component spins that are randomised due to the various interactions. Thus, effective inspiral values are expected to be symmetrically distributed around zero [11,12].

The effective inspiral spin, χ_{eff}, is a valuable parameter for distinguishing between binary black hole formation channels. It is defined as

$$\chi_{\text{eff}} = \frac{m_1\chi_1 \cdot \hat{L} + m_2\chi_2 \cdot \hat{L}}{m_1 + m_2}$$

where m_1 and m_2 are the primary and secondary component masses, $\vec{\chi}_1$ and $\vec{\chi}_2$ are the dimensionless spin vectors of each black hole with magnitudes between 0 and 1, and $\hat{L}$ is the unit vector along the orbital angular momentum of the system.

This measurement can be defined as the mass-weighted projection of the individual spins onto the orbital axis, which effectively captures the degree of spin alignment in the system. The distribution of χ_{eff} within a population is what provides key information about its formation history. Binaries that are formed through isolated binary evolution are likely to have spins aligned with the orbit, which results in larger positive χ_{eff} values [13]. On the other hand, dynamically assembled binaries have spin orientations are randomised by the dense stellar environment, exhibiting distributions symmetric around zero [11]. Thus, comparing the χ_{eff} distributions for mass-gap mergers and the broader black hole population offers a way to constrain the astrophysical processes responsible for their formation.

This study focuses on identifying and analysing gravitational-wave merger events with at least one component mass within the 2.5 to 5 $M_\odot$ range. The study seeks to provide a systematic comparison of χ_{eff} distributions for mass-gap mergers relative to those of higher-mass black hole binaries. This work therefore contributes to the ongoing effort to understand how the compact objects of the lower mass gap form, helping to clarify whether their presence points to unusual stellar evolution or alternative astrophysical processes.

Previous gravitational-wave catalogues have already provided valuable insights into black hole populations and spin characteristics. The first catalog, GWTC-1 [14], reported many binary black hole mergers with effective inspiral spins clustered near zero, suggesting predominantly isotropic spin orientations consistent with dynamical formation scenarios. The GWTC-2 catalog [15]expanded the sample events and again showed that most binaries exhibit low spin magnitudes, though a few events had minimal spin alignment. With the release of GWTC-3 [16], more candidate events were introduced, some with component masses in the lower mass gap. This provided the statistical evidence that compact objects in this range exist, creating an opportunity to investigate their properties further. This motivates the present study, which aims to investigate the spin properties of mass-gap black holes to better understand their astrophysical origins.

Previous Works

The spin distributions of merging black holes have been a key focus of gravitational-wave population studies. As mentioned previously, analyses of GWTC-1 [14]and GWTC-2 [15] found that most binaries have effective inspiral spin parameters (χ_{eff}) consistent with zero, implying largely isotropic spin orientations and supporting dynamical assembly in dense stellar environments. However, there were still events with small positive values, suggesting instances of isolated binary evolution with weak alignment. The existence of compact objects within the lower mass gap has been investigated by several authors. Gayathri, V. et al [17] investigated hierarchical black hole mergers, a merger where at least one of its black holes was formed from a previous merger. Using Bayesian analysis, it was found that GW170817A had high mass and spin that strongly favoured the scenario.

Theoretical studies have also explored how different formation channels affect spin distributions. Rodriguez et al. [18] demonstrated that dynamically assembled binaries in globular clusters should exhibit spin orientations that are isotropic, producing χ_{eff} values symmetrically distributed around zero. It modelled how black holes in dense star clusters can undergo repeated mergers, forming increasingly massive "second-generation" black holes. This was done through 96 dynamical model simulations with varying initial spin assumptions. The results highlight that the observed mass and spin distributions of gravitational-wave sources depend strongly on the birth spins of stellar-origin black holes. In contrast, isolated binary evolution models predict preferentially aligned spins and positive χ_{eff} values. Despite these advances, few studies have focused specifically on the spin properties of binaries containing lower mass-gap components. Therefore, this study aims to extend previous analyses by systematically comparing the effective inspiral spin distributions of lower mass-gap mergers, providing new insight into their formation pathways.

Observational data

The analysis uses the publicly available posterior samples from the GWOSC catalogue, [7–9] extracting the component mass and χ_{eff} data for each event. The chosen samples were from the most up-to-date GWTC-3 releases [19] . To construct the dataset, all events from the GWTC-3 catalogue were first searched for component masses within the range of 2.5 to 5 $M_\odot$. The extended upper limit was chosen to ensure that potential mass-gap candidates with larger measurement uncertainties were not prematurely excluded. This range captured

systems whose credible intervals overlap with the real lower mass gap.

For each candidate, the probability of each component mass lying within the real lower mass gap was then computed by dividing the number of posterior samples within the range by the total number of samples. Events with at least one component having a posterior probability greater than 40% were retained. The 40% threshold was selected as a compromise between a lower threshold that risks admitting events with negligible prominence in the gap and a high threshold that would exclude events with posterior distributions that are only partially overlapped due to measurement uncertainty. Alternative thresholds between 20% and 60% were also tested. Below a 40% threshold admitted events with large uncertainties, whilst higher thresholds further reduced an already limited sample size and left too few events to support meaningful conclusions. Therefore, the 40% threshold was a practical balance. This criterion was necessary as many events in the catalogue had large bounds of uncertainties for several events.

In total, nine events met all the criterias and were included in the final analysis. Table 1 lists each selected event, the component masses, and the probability of each component lying within the mass gap.

Event	Mass 1	Mass 2	P(Mass 1)	P(Mass 2)
GW190814_211039	23.3	2.6	0.000	0.925
GW200210_092254	24.1	2.83	0.000	0.896
GW190821_124821	8	3.9	0.017	0.745
GW190704_104834	5 (-2)	3.1	0.084	0.689
GW190920_113516	4 (-3)	2.8	0.156	0.589
GW190910_012619	34	3.2	0.000	0.580
GW190924_021846	8.8	3.5 (-1.5)	0.000	0.433
GW190930_133541	18	5	0.001	0.403
GW230529_181500	3.6	1.4	0.923	0.000

Table 1

Methodology

This study investigates the formation channels of binary black holes within the lower mass gap using gravitational-wave observations. I analyse the publicly available data from the GWTC released by the LIGO–Virgo–KAGRA (LVK) collaboration[5,6,20]. The analysis focuses on the component masses and the effective inspiral spin parameter, $\chi_{\rm eff}$, which is sensitive to the alignment of black hole spins and provides a key diagnostic of formation pathways.

The population distribution of $\chi_{\rm eff}$ for mergers in the lower mass gap is inferred and compared with theoretical predictions for different black hole formation channels[21]. For each selected event in the GWTC, posterior samples $\{\chi_{\rm eff}^{(i)}\}$ indexed by i are used. The population distribution of $\chi_{\rm eff}$ is modeled as a Gaussian with mean μ and standard deviation σ, which are the parameters to be inferred. A uniform prior on μ over $[-1,1]$ and a half-normal prior on σ, corresponding to a normal distribution with mean zero and unit variance truncated to positive values. Assuming the population distribution is Gaussian, the likelihood of the selected GWTC events is

$$\begin{aligned}\mathscr{L}(\{\chi_{\rm eff}^{(i)}\}\mid\mu,\sigma) &= \prod_i \mathscr{L}(\chi_{\rm eff}^{(i)}\mid\mu,\sigma)\\ &= \prod_i \frac{1}{N_i}\sum_j \mathscr{L}(\chi_{\rm eff}^{(i,j)}\mid\mu,\sigma)\end{aligned}$$

where independence of events implies a product over i. The final expression leverages posterior samples: the likelihood for each event is estimated by averaging over its N_i posterior samples, with $\chi_{\rm eff}^{i,j}$ denoting the j^{th} sample of the i^{th} event. Finally, I have that the likelihood of a single posterior sample is

$$\mathscr{L}(\chi_{\rm eff}^{(i,j)}\mid\mu,\sigma) = \frac{1}{\sigma\sqrt{2\pi}}\exp\left[-\frac{(\chi_{\rm eff}^{(i,j)}-\mu)^2}{2\sigma^2}\right]$$

Thus, μ denotes the population mean of the effective spin, with $\mu > 0$ indicating preferential alignment, $\mu < 0$ anti-alignment, and $\mu \approx 0$ consistency with isotropy. The parameter σ captures the dispersion: small values imply a tightly clustered $\chi_{\rm eff}$ distribution, while large values indicate greater variability in $\chi_{\rm eff}$. I sample the posterior distribution of (μ,σ) using the Markov Chain Monte Carlo (MCMC) algorithm implemented in emcee[22]. To assess convergence, I compute the Gelman–Rubin diagnostic $\hat{R}$ for both parameters[23]. This statistic compares the variance between multiple Markov chains to the varience within each chain (between-chain and within-chain). Values that are close to unity indicate that the chains have mixed well and are sampling from the same posterior distribution. Traditionally, $\hat{R} < 1.1$ has been considered sufficient for convergence, but more recent works recommend a more stringent threshold of $\hat{R} < 1.01$ to ensure robust mixing[23]. Therefore, I used $\hat{R} < 1.01$ as the convergence criterion for both parameters.

Results

The primary aim of this work was to investigate the distribution of the effective inspiral spin parameter $\chi_{\rm eff}$ in compact object mergers containing at least one component within the lower mass gap range of 2.5 to 5 $M_\odot$. Using posterior samples from the GWTC-3 catalogue[19], I applied population-level inference to estimate the mean (μ) and standard deviation (σ) of $\chi_{\rm eff}$ across this subset of events. The histogram of the inferred mean $\chi_{\rm eff}$ —denoted μ —indicates that the population mean is consistent with zero within statistical uncertainties:

$$\mu = 0.028^{+0.069}_{-0.049}, \quad \sigma = 0.094^{+0.190}_{-0.061}$$

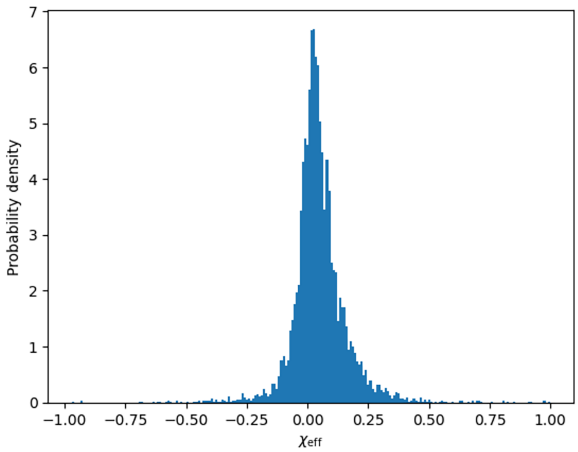

Fig. 1 Histogram showing the distribution of effective inspiral spin parameter for compact objects in the lower mass gap. The distribution appears to be centered near zero, consistent with isotropic spin orientations.

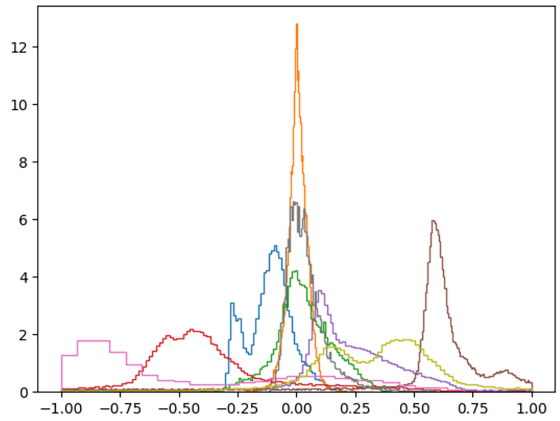

Fig. 2 Split histogram showing each sampled event.

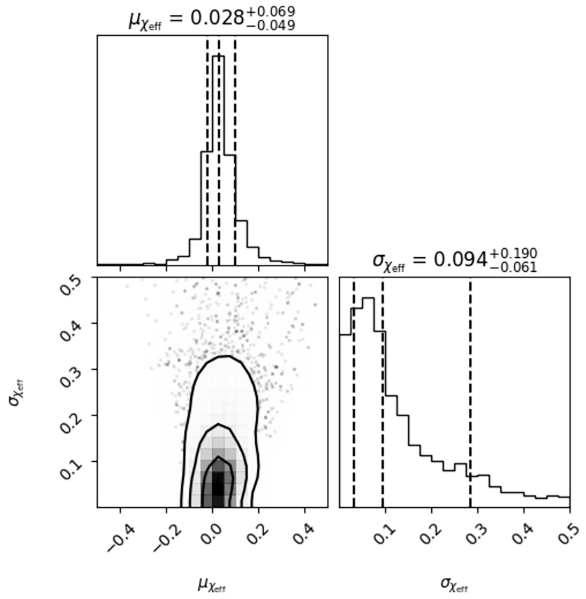

Fig. 3 Corner plot showing the two-dimensional posterior distribution of the population parameters μ and σ for the effective inspiral spin. The contours reveal a mild degeneracy between the mean and standard deviation parameters. This is an important result, as $\chi_{\rm eff} \approx 0$ is a hallmark of isotropic spin-orbit orientations, which are more typical of dynamically assembled systems than of binaries formed through isolated stellar evolution[11]. Additionally, the two-dimensional posterior distribution of μ and σ reveals a mild degeneracy. As μ increases, σ tends to decrease, and vice versa. The corner plot illustrates this behaviour clearly, with contour lines enclosing progressively higher percentages of posterior probability. The contours themselves are relatively symmetric, suggesting that the degeneracy is modest but still present.

In this analysis, the population distribution of the effective inspiral spin parameter $\chi_{\rm eff}$ is modelled as a Gaussian with mean μ and standard deviation σ. This choice is not intended to provide an exact physical description of the underlying spin distribution. In realistic astrophysical scenarios, different binary formation channels may produce $\chi_{\rm eff}$ distributions that are intrinsically skewed or uneven. However, the present sample contains only a small number of merger events with at least one component in the lower mass gap, and individual measurements have substantial posterior uncertainties. As a result, introducing additional shape parameters would be weakly constrained and susceptible to overfitting. Additionally, when posterior samples from the many independent events are combined, event specific asymmetries are effectively marginalised over. In this regime, the aggregated population likelihood is expected to be smooth and approximately symmetric. For this reason, a Gaussian approximation can be justified. This reasoning is consistent with expectations from the Central Limit Theorem and applies to the combined population inference rather than to individual event posteriors. An inspection of individual events highlights certain outliers. One merger event exhibits a posterior peaked near $\chi_{\rm eff} \approx -1$ (the pink event in the figures). Given that $\chi_{\rm eff} = -1$ corresponds to maximally anti-aligned spins, such a configuration is impossible to produce in isolated binary evolution scenarios, where forces and mass transfer tend to align spins with the orbital angular momentum[13]. Instead, this event is most naturally explained as the product of a dynamical capture in a dense stellar environments such as a globular cluster or nuclear star cluster[12].

At the other extreme, events with $\chi_{\rm eff}$ close to $+1$, though less common in the subset, would strongly suggest isolated binary formation, as they imply nearly maximally aligned spins. Only a single event falls near $+1$. This event is GW190920 and has component masses of 7 and 2.8. This event could po-

tentially be a case of isolated binary evolution and an anomaly. However, there is also the possibility that it is an extreme case of dynamical assembly. To assess this quantitatively, I estimated the probability of obtaining similarly large values of $\chi_{\rm eff}$ under the isotropic spin distribution. Using the posterior samples of GW190920, the probability of exceeding posterior median was found to be 9.89%, while the probability of exceeding a 90% lower bound was approximately 47%. These values $\chi_{\rm eff} \approx 0$ that this event is not statistically rare under isotropic spin assumptions. Therefore, there is not enough evidence to unequivocally support one formation channel. Nevertheless, the majority of events cluster near 0 reinforcing the interpretation of isotropic spin distributions.

Resampling

The credible intervals on the parameters μ and σ are relatively wide compared to their mean values and reflect the limited number of events in the lower mass gap. To assess the sensitivity of the inferred trends to individual events' uncertainties, a jackknife resampling analysis was performed. In this test, the population inference was repeated multiple times, each time removing a single event recalculating the parameters μ and σ using the remaining samples.

Excluded Event	μ	σ
GW190814_211039	0.67505960	0.32221158
GW200210_092254	0.03947047	0.36428733
GW190821_124821	-0.00299713	0.35695343
GW190704_104834	0.03070033	0.18982736
GW190920_113516	0.02682440	0.25389265
GW190910_012619	-0.00350918	0.18411201
GW190924_021846	0.05340567	0.20360489
GW190930_133541	0.00501970	0.28543173
GW230529_181500	0.13190350	0.22058217

Table 2

The jackknife results indicate that the inferred value of μ is moderately sensitive to the exclusion of individual events. While the majority of jackknife realisations yield μ values clustered near zero, one resampled dataset, exclusion of GW190814_211039, produces a substantially larger value of μ, indicating that the single event carries a larger leverage compared to the other. Nevertheless, the full-sample estimate of μ remains small and consistent with zero within its credible interval. The inferred population width σ exhibits a larger relative variation across the jackknife samples, as expected given the small sample size. This behaviour suggests that while the precise value of μ is weakly constrained, the overall scale of the population width is not dominated by a small subset of events. Importantly, removing events with posterior support near extreme $\chi_{\rm eff}$ values does not qualitatively alter the inferred population parameters. This demonstrates that such events do not exert a disproportionate influence on the population-level inference, as seen by the figures 4-12. Therefore, the jackknife resampling provides a consistency check, confirming that the inferred population trends are robust to the exclusion of any single merger.

Considering these results, individual events with $\chi_{\rm eff}$ values near ± 1 should be interpreted with caution. Their posterior distributions remain broad, and their credible intervals typically include substantially lower absolute values of $\chi_{\rm eff}$. While such events are consistent with specific formation scenarios, including dynamical assembly or isolated binary evolution, the present data do not allow them to be classified as physically distinct outliers rather than statistical variations within a small sample. Overall, the jackknife resampling supports the conclusion that the population mean μ is consistent with zero within current uncertainties, while highlighting that larger samples will be required to more tightly constrain the population width and to assess the physical significance of extreme $\chi_{\rm eff}$ events.

Discussion & Analysis

Implications and Significance

The central implication of a population mean $\chi_{\rm eff}$ consistent with zero is that the average individual spin orientations in these mergers are isotropic. This is a critical distinction between formation channels:

- Isolated binary evolution tends to produce aligned spins ($\chi_{\rm eff} > 0$) because both stars originate from the same molecular cloud and experience tidal alignment before collapse [16].
- Dynamical assembly (e.g., in globular clusters, nuclear star clusters) produces isotropic spin distributions, as measured, as the binary components are brought together through numerous random gravitational encounters [11,12].

The observed isotropic distribution observed in the results implies that majority of the compact objects in the lower mass gap originate from dynamical assembly. Dynamical assembly inherently requires a pre-existing population of black holes in a dense environment. These black holes eventually undergo gravitational encounter, causing the mergers. While the inferred population mean $\chi_{\rm eff}$ is consistent with zero, this result does not uniquely imply isotropic spin orientations. Low values of $\chi_{\rm eff}$ arise from a fundamental degeneracy between spin orientation and spin magnitude. In particular, binaries with nearly aligned spins but small spin magnitudes would

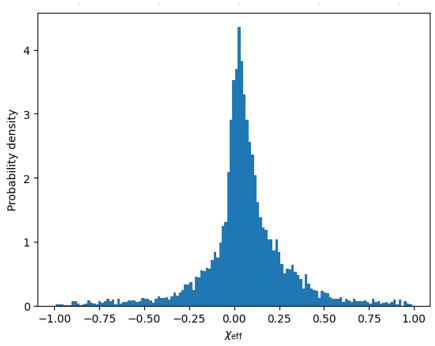

Fig. 4 GW190814_211039

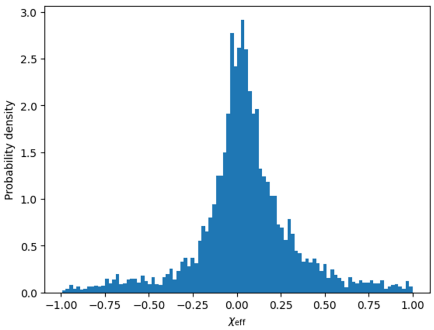

Fig. 5 GW200210_092254

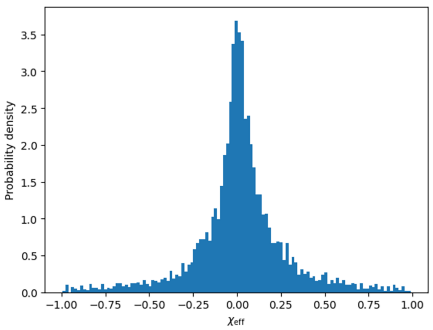

Fig. 6 GW190821_124821

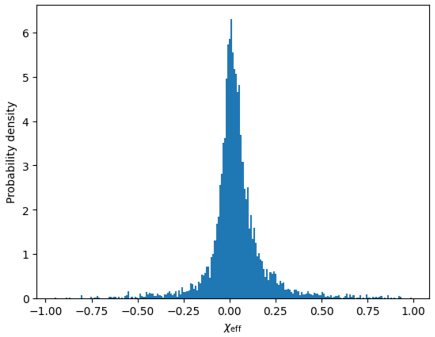

Fig. 7 GW190704_104834

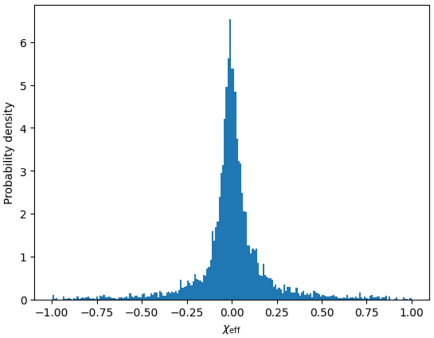

Fig. 8 GW190920_113516

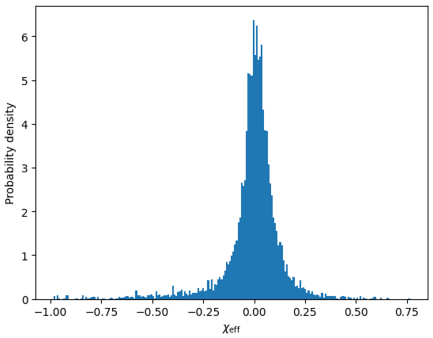

Fig. 9 GW190910_012619

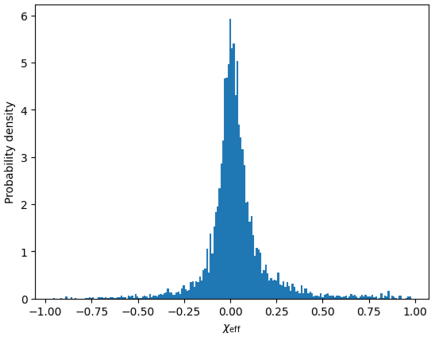

Fig. 10 GW190924_021846

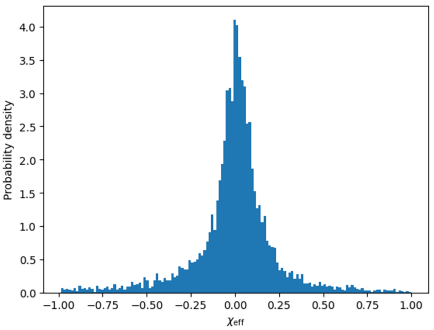

Fig. 11 GW190930_133541

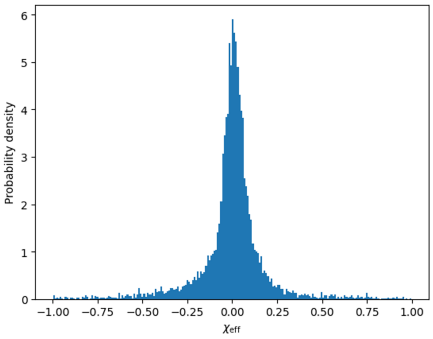

Fig. 12 GW230529_181500

also present $\chi_{\rm eff}$ values near zero. As a result, a population of weakly spinning binaries may potentially be indistinguishable from a population with larger but isotropic spins when considering $\chi_{\rm eff}$ alone. The Gaussian population model used therefore captures the symmetry of the distribution but does not distinguish the contributions of spin magnitude and spin tilt. The consistency of μ with zero indicates the absence of a strong preference for positive or negative $\chi_{\rm eff}$ values. However, it cannot by itself discriminate between isotropic spin orientations and low spin systems. Additional information would be required for differentiating. In this context, the present results should be interpreted as evidence against strongly aligned populations, rather than as definitive proof of isotropic spin orientations.

Two distinct scenarios can explain the source of the original compact objects in these mergers. Firstly, black holes formed from isolated stellar evolutions could enter dense environments. These external black holes independently form from the collapse of massive stars (typically with masses of $20-25\,M_{\odot}$) and can migrate into or form within dense stellar environments. In these environments, the black holes would interact and merge with other compact objects in the environment.

An alternative scenario that could be explored in future work involves the existence of primordial black holes. Unlike stellar black holes, primordial black holes are hypothesised to have formed directly in the early Universe. If primordial black holes exist in sufficient numbers, they could form a dense cluster that later create or merge with stellar systems. This scenario enables dynamical assembly to occur much earlier than possible with stellar-origin black holes. Primordial black hole mergers would also exhibit isotropic spin distributions, which is consistent with the $\chi_{\rm eff} \approx 0$ observed in this study[24]. Their inclusion here should therefore be viewed as a speculative but interesting avenue for future investigation. Further observational and theoretical studies would be required to determine whether primordial black holes could play a measurable role in shaping the population of compact objects within the lower mass gap. While observational evidence for significant primordial black hole populations remains scarce, the isotropic spin distribution observed in the lower mass gap mergers is compatible with either scenario.

Recommendations

Future work on the effective inspiral spin distribution of mergers involving mass-gap components would benefit from several methodological and observational improvements. Firstly, increasing the sample size is crucial. As future observing runs expand the GWTC catalogue, the number of events meeting the selection criteria will grow, allowing for narrower statistical uncertainties on both the mean (μ) and standard deviation (σ) of $\chi_{\rm eff}$. A larger dataset will also reduce the influence of outliers and help confirm whether the clustering near $\chi_{\rm eff} \approx 0$ persists.

Secondly, refining the event classification could significantly improve the robustness of the inferences. Instead of imposing a strict posterior probability threshold for identifying mass-gap components, hierarchical Bayesian models could simultaneously fit for the $\chi_{\rm eff}$ distribution and the likelihood that a given event contains a mass-gap object. This would better account the classification uncertainty and avoid potential biases if misclassified events have systematically different spin properties.

Limitations

The principal limitation of this study is the small number of events meeting in the mass-gap selection criteria. With only a handful of mergers contributing to the posterior, the credible intervals on μ and σ remain quite broad and can cause significant influence from outliers. The use of a 40% posterior probability threshold for mass-gap classification introduces uncertainty in sample composition and could bias the inferred population parameters if misclassified events have systematically different $\chi_{\rm eff}$ values.

The discussion of primordial black holes also remains speculative. Whilst $\chi_{\rm eff} \approx 0$ is compatible with primordial black holes contribution, it is also consistent with dynamical assembly of stellar-origin black holes. It is important to note that primordial black holes are not an alternative to dynamical assembly but a possible subset of objects participating in it: dynamical assembly requires pre-existing black holes that were not formed via isolated binary evolution, and primordial black holes would satisfy that requirement if they exist.

Without additional observables, such as mass function shape, redshift distribution, or eccentricity, it is not possible to distinguish between these possibilities. Among potential parameters, the mass ratio q of merging binaries is a promising diagnostic for differentiating between formation routes. Dynamical assembly in dense stellar environments tends to produce binaries with comparable component masses (typically $q \geq 0.5$), as repeated exchange interactions—three-body gravitational encounters in which a more massive black hole replaces the lighter object—preferentially eject lower-mass objects and retain heavier ones[25]. This process naturally makes dynamically formed binaries have near equal masses. In contrast, isolated binary evolution can lead to more unequal mass ratios. This can be due to the component masses being determined by the initial stellar mass function (IMF), the distribution of stellar birth masses which favours low mass stars. Within the binary, one star expands and transfers material to its companion during evolution through mass transfer episodes. Thus, depending on the stability and efficiency of mass ex-

change, the final mass ratios can vary significantly. Future work could focus on modelling q and χ_{eff} distributions to assess whether the observed population favours symmetric mass distribution as predicted in dynamical assembly or the broader distribution for isolated binary evolution, which would contrast this study's findings. Such approach would provide more testing of the competing formation scenarios.

Conclusion

This study presents a systematic analysis of the effective inspiral spin distributions of gravitational-wave mergers containing compact objects within the lower mass gap from 2.5 to 5 $M_{\odot}$. The findings indicate that the effective spins of these systems cluster near zero, implying that their spin orientations are largely isotropic. Such a distribution is most consistent with binaries formed through dynamical interactions in dense stellar environments, where repeated gravitational encounters randomise spin directions.

This interpretation contrasts sharply with expectations from isolated binary evolution, which tends to produce aligned spin configurations and positive effective spin values. The presence of events with strongly anti-aligned spins further supports the role of dynamical assembly, as such configurations are difficult to achieve through isolated stellar evolution alone. Together, these findings suggest that the lower mass gap is primarily populated by dynamically assembled systems rather than binaries formed through standard stellar evolution pathways. The implications of this result extend beyond identifying formation channels. Dynamical assembly requires pre-existing populations of compact objects within dense environments, implying that black holes in this mass range likely originate from earlier generations of mergers or from primordial black holes. The observed isotropic spin orientations are therefore compatible with both stellar-origin and primordial black hole scenarios. The latter, though maintained as a plausible case in this study, is not yet confirmed.

By establishing an understanding of near-zero effective spins in the lower mass gap, this study strengthens the evidence for dynamical formation as a key mechanism shaping the compact object population. Future observing runs of the LIGO-Virgo-KAGRA will expand the catalogue of detected mergers, enabling more precise constraints on spin distributions, allowing researchers to test whether the observed isotropy persists across different mass ranges.

References

1 A. Heger, *The Astrophysical Journal*, 2003-07, **591**, 288.
2 C. D. Bailyn, *The Astrophysical Journal*, 1998-05, **499**, 367–374.
3 F. Özel, *The Astrophysical Journal*, 2010-12, **725**, 1918–1927.
4 C. L. Fryer, *The Astrophysical Journal*, 2012-04, **749**, 91.
5 B. Abbott, *Phys. Rev. Lett*, 2016-02-06, **116**, 061102.
6 Acernese, *Classical and Quantum Gravity*, 2014-12, **32**, 024001.
7 *The LIGO Scientific, the Virgo Collaboration, and the KAGRA Collaboration. Open Data from LIGO, Virgo, and KAGRA through the First Part of the Fourth Observing Run*, 2025, https://arxiv.org/abs/2508.18079., arXiv: 2508.18079 [gr-qc].
8 A. R., *Open Data from the Third Observing Run of LIGO, Virgo, KAGRA, and GEO"*, 2023-07.
9 A. R., *Open data from the first and second observing runs of Advanced LIGO and Advanced Virgo"*, 2021.
10 K. Belczynski, D. Holz, T. Bulik and R. O'Shaughnessy, *Nature*, 2016-06, **534**, 512–515.
11 C. L. Rodriguez, *Binary Black Hole Mergers from Globular Clusters: Implications for Advanced LIGO"*, 2015-07-05.
12 S. F. Zwart and S. L. McMillan, *The Astrophysical Journal*, 2002-09, **576**, 899 907.
13 V. Kalogera, *Spin-Orbit Misalignment in Close Binaries with Two Compact Objects"*, 2000-09, /309400. arXiv: astro - ph / 9911417.
14 Abbott, *GWTC-1: Observations of Gravitational Waves from Compact Binary Coalescences*, 2019-09-03.
15 Abbott, *GWTC-2: Compact Binary Coalescences Observed by LIGO and Virgo During the First Half of the Third Observing Run*, 2021-03-02.
16 Abbott, *GWTC-3: Compact Binary Coalescences Observed by LIGO and Virgo During the Second Part of the Third Observing Run*, 2021-11, https://arxiv.org/pdf/2111.03606., arXiv preprint arXiv:2111.03606.
17 V. Gayathri, *The Astrophysical Journal Letters*, 2020-02, **890**, 20.
18 Rodriguez, *Physical Review*, 2019-08, **100**, 043027.
19 R. Abbott, *Physical Review*, 2023-10, **13**, 041039.
20 K. Collaboration, *Nature Astronomy*, 2019-01, **3**, 35–40.
21 S. Stevenson, C. P. Berry and I. Mandel, *Monthly Notices of the Royal Astronomical Society*, 2017-07, **471**, 2801–2811.
22 D. Foreman-Mackey, *emcee: The MCMC Hammer*, Mar. 2013), record ascl:1303.002.
23 A. Gelman and D. B. Rubin, *Statistical Science*, 1992-01, **7**, 457–472.
24 B. Carr and F. Kühnel, *Annual Review of Nuclear and Particle Science*, 2020, **70**, 355–394.
25 F. Antonini and F. A. Rasio, *The Astrophysical Journal*, 2016-11, **831**, 187.